* 1998 Alfred L. Hendry Award Winner *

The purpose of the Southern Society Alfred L. Hendry Memorial Award is to encourage undergraduate college and university students to do work in and author papers in some aspect of coatings technology.

The award consists of $1,000, expenses covering attendance at the FSCT Annual Meeting and International Coatings Expo to receive the award, and a suitably inscribed plaque for the best paper submitted during the award year.

The award was established in 1986, by the Southern Society for Coatings Technology as sponsors, in memory of an honored Past-President of the Society, Alfred L. Hendry.

Chlorinated Maleinized Guayule Rubber as an Adhesion Promoter for Polypropylene

Michael D. Foster† and Shelby F. Thames*—The University of Southern Mississippi

Chlorinated maleinized guayule rubbers (CMGR) were synthesized and applied as coatings onto polypropylene panels. CMGR orientation was critical to adhesion and was verified by contact angle measurements. Reducing the quantity of tetrahydrofuran (THF) decreased adhesion from 57 N/cm^2 with pure THF to 23 N/cm^2 with four percent THF in water. Percent maleinization above a critical concentration of 15 by weight decreased adhesion. However, 10% maleinization was required for dispersion stability in water while 5-10% concentration provided maximum adhesion. A five percent maleic CMGR dispersion at 240 g/L THF concentration was stable for less than 24 hr while a 10% maleic anhydride concentration has shown long-term stability.

INTRODUCTION

Waterborne coatings employ additives to lower surface tension and improve substrate wetting. However, these additives have little effect on adhesion to very low energy surfaces such as polypropylene (PP) or polyethylene. Wetting and adhesion to these surfaces must then be improved by other means. This problem is exacerbated by a trend towards low volatile organic compound (VOC) waterborne coatings.

The work of adhesion has been defined as interfacial tension between two surfaces after curing plus covalent bond energy.[1,2] Surface tension (γ_{total}) can be resolved as dispersive ($\gamma_{dispersive}$), polar or Lewis acid-base (γ_{polar}), and hydrogen bonding (γ_h) forces [see equation (1)].

$$\gamma_{total} = \gamma_{dispersive} + \gamma_{polar} + \gamma_h \quad (1)$$

Fowkes' equation (2)[3] for adhesion (W_a) relates contact angle "theta" (Θ) of a liquid with surface tension equal to γ_L to dispersive (d), polar acid-base (a,b), polar base-acid (b,a), and hydrogen (h) bonding ability of surface (S) and liquid (L):

$$W_a = 1 + \cos\Theta = \frac{1}{2}\left(\sqrt{\gamma_L^d + \gamma_S^d} + \sqrt{\gamma_L^a + \gamma_S^b} + \sqrt{\gamma_L^b + \gamma_S^a} + \sqrt{\gamma_L^h + \gamma_S^h}\right) \quad (2)$$

Low energy surfaces lack polar groups and thus adhesion is solely confined to the Van der Waals, or dispersive adhesion forces.[1]

Van der Waals' forces can be classified into dipole and London forces. London force, the least of the Van der Waals interactions, produces only weak interaction with substrate surface molecules and a low adhesive strength. However, since London forces are conveyed by electrons and protons, atoms of high electron density produce the largest London force. Chlorine has a unique combination of large electron affinity and minimal atomic radius, yielding near maximum London force development ability with a high electron density per volume. Chlorine is also very electronegative, creating permanent dipolar bonds[4] and adding the ability to induce dipolar attraction within a contacting surface.[5]

Current adhesion promoting technologies use chlorine[6] or sulfur[7] for adhesion promotion to low energy surfaces. In addition, a number of waterborne technologies have been used to apply chlorinated (CPOs) and non-chlorinated polyolefins[8,9] to nonpolar surfaces such as PP. Other than one very recent patent,[10] no other

*Box 10037, Hattiesburg, MS 39406-0037, E-mail: Shelby.F.Thames@usm.edu.
†Box 10076, Hattiesburg, MS 39406-8500.

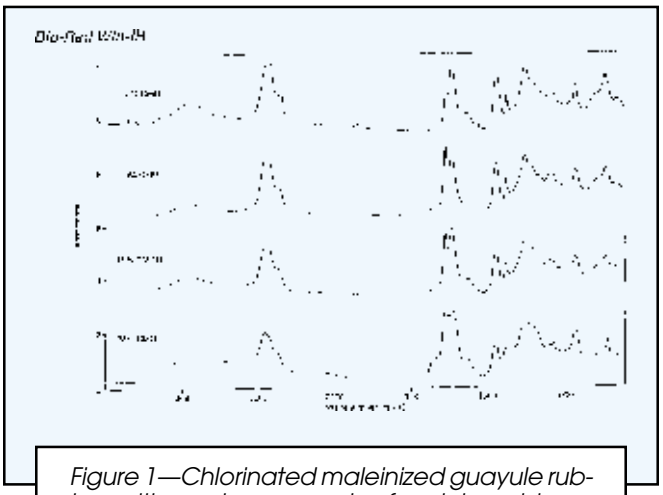

Figure 1—Chlorinated maleinized guayule rubber with varying amounts of maleic acid.

Table 1—List of Coatings Formulations

	25 % VOC	4 % VOC	75% VOC (Solventborne)
CMGR	1g	1g	2.5g
THF	25g	4g	6.5g
mEA-nOH	0.5g	0.5g	0.5g
	m=3, n=0	*	m=2, n=1
DI water	73g	94g	0g
Surfactant	0.5g	0.5g	0.5g
Total	100g	100g	10.0g

*Note: diethylaminoethanol, ethylaminodiethanol, and triethanolamine (m=2, n=1; m=1, n=2,; and m=0, n=3, respectively) used independently with each percent maleic anhydride.

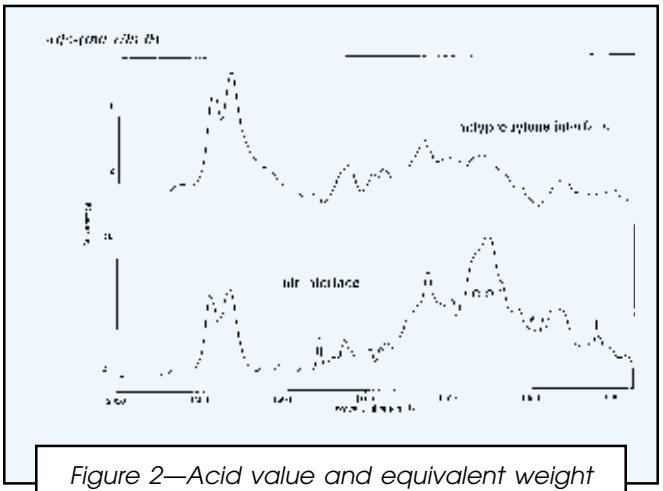

Figure 2—Acid value and equivalent weight as a function of percent maleic anhydride.

attempt to synthesize a self-dispersing chlorinated adhesion promoter has been successfully demonstrated.

Chlorinated maleinized guayule rubber (CMGR) was examined as a waterborne adhesion promoter (AP) for PP. The target formulation was designed to be compliant with "Rule 632," limiting VOC content to below 40%.[11] Adhesive interfaces were characterized by contact angle analysis, pull-off adhesion, and FTIR techniques. CMGR dispersion stability in water was assessed by the time required for phase separation as a function of maleinization. The strength of adhesion was maximized by modeling the best drying procedure and optimum concentration of maleic content through experimental design. Finally, the effects of solvent content and percent maleinization were explored by comparing the adhesive properties of three different VOC formulations, two waterborne and one analogous solventborne.

EXPERIMENTAL

Materials and Equipment

CMGR was synthesized by a procedure outlined by Purvis and Thames, 1996.[12] All chemicals were obtained from Aldrich and used as received unless otherwise noted. Octylphenoxypoly (ethyleneoxy) ethanol, tradename CA630, was obtained from Rhone-Poulenc. Attenuated total reflectance, Fourier transform infrared absorbance spectra (ATR FTIR) were collected using a BioRad FTS-25 equipped with a Harrick variable angle ATR attachment and a 45° germanium crystal. PP panels, from McMaster-Carr having density .90-.91 g/cc, tensile strength of 3200-5300 psi, 330-335°F softening temp, and hardness of 60-75 (D scale) by Shore method, were cleaned with a series of solvents; methylene chloride, acetone, and deionized water, in respective fashion. Each panel was then air dried 30 min. The adhesion promoter coating was then applied using a doctor blade of 1 mil gap. Adhesive strengths were measured on a Material Testing System MTS 810 with 458.20 controller and 458.51 microprofiler driven by Testworks 2.1 software according to ASTM D 4541. Contact angles were measured using a First Ten Angstroms FTÅ 200 digital video contact angle instrument and version 3.01 software. Analysis of variables was mathematically solved by experimental design (Design-Expert 4.0.8C) software.

FTIR Analysis of CMGR

Percent maleinization was examined by FTIR absorption spectra. Solid powder samples were combined with KBr, pelletized, and analyzed for infrared absorption. The spectra were height normalized to a maximum peak size. Peaks giving rise to the anhydride and free acid were qualitatively compared against the aliphatic peaks from the rubber backbone.

Titration of CMGR

Percent maleinization was further checked by titration of samples for their acid values. Each sample (~1g) was dissolved in 100 mL of dimethylsulfoxide (DMSO)

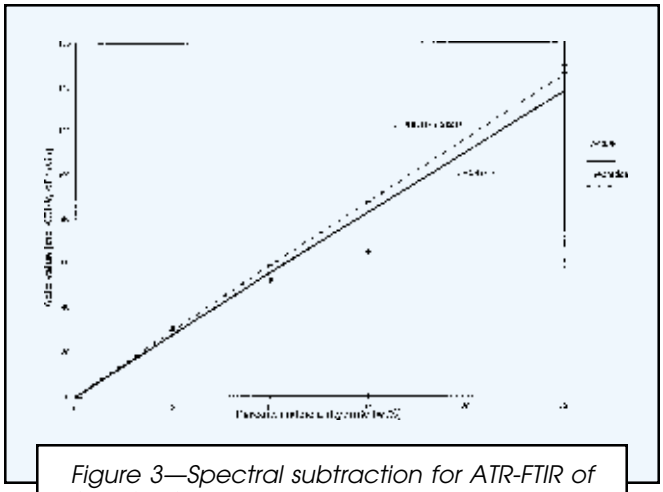

Figure 3—Spectral subtraction for ATR-FTIR of 25% CMGR.

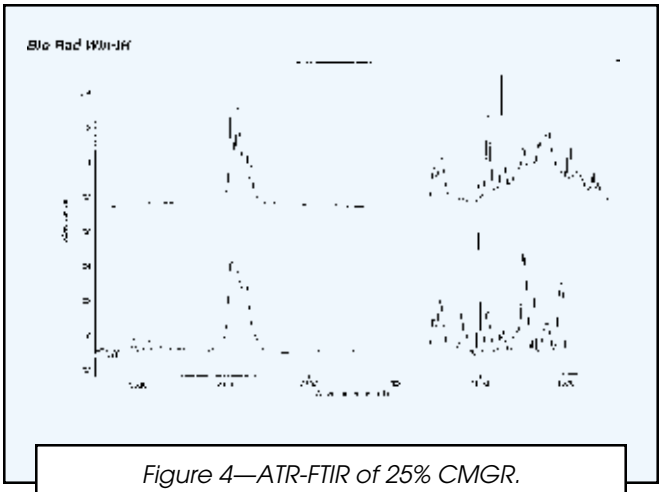

Figure 4—ATR-FTIR of 25% CMGR.

and titrated against a 0.1037 M solution of methanolic potassium hydroxide using phenolphthalein indicator. Upon reaching the titration equivalence point, CMGR precipitated. Acid values were plotted against theoretical maleic anhydride content.

Coating Formulation

The adhesion promoting polymer was formulated into a waterborne coating. Powdered CMGR was dissolved in tetrahydrofuran (THF) and trace water, and the free acids were neutralized by the addition of an organic base, triethylamine. After 30 min deionized water was slowly added with vigorous stirring to produce a 1%W/W CMGR solution. Coating ingredients are listed in *Table* 1.

VOC Effect on Adhesion

The THF content was further decreased by adding ethanoldiethylamine, diethanolethylamine, or triethanolamine, then reduced with deionized water to four percent VOC. Finally, a solventborne formulation of CMGR consisted of a 25%W/W CMGR dissolved in THF with a 1.5X stoichiometric amount of water for hydrolysis of anhydride to the free acid.

Surface Application

Coatings were drawn down on PP panels at 250nm thickness using a doctor blade of 25 µm (1 mil), then raised on end to prevent surface pooling. The PP coated panels were devolatilized in an oven using time and temperature parameters outlined in the experimental design. Default cure parameters were 100°C for 20 min. Finally, all panels were allowed to cool to ambient temperature.

Coating Surface Analysis

The difference in chemical composition of the coating between the air and substrate interfaces was investigated by ATR FTIR and contact angle. Absorbance spectra were collected of the air and PP interfaces against a 45° germanium crystal to minimize depth of penetration. Spectral subtraction was performed to examine component migration within the coating to the air of PP interface.

Experimental Design

An experimental design was set up to test the variables %W/W maleic acid, baking temperature, and bake time. The –1, 0, and 1 level parameters of each variable were as follows: 5, 15, and 25%W/W maleic content; 100, 10, and 120°C; and 20, 160, and 300 min, respectively. The experimental responses modeled pull-off adhesive strength and surface contact angle with models plotted over the design space.

Adhesion Testing

Aluminum dollies, obtained from Paul N. Gardner, were adhered to the panel surface with JB Weld epoxy glue. The removal force to pull the dolly from the surface was recorded (ASTM D 4541). Force values were computed by dividing the average pull-off force in Newtons by the dolly surface area (3.14 cm^2).

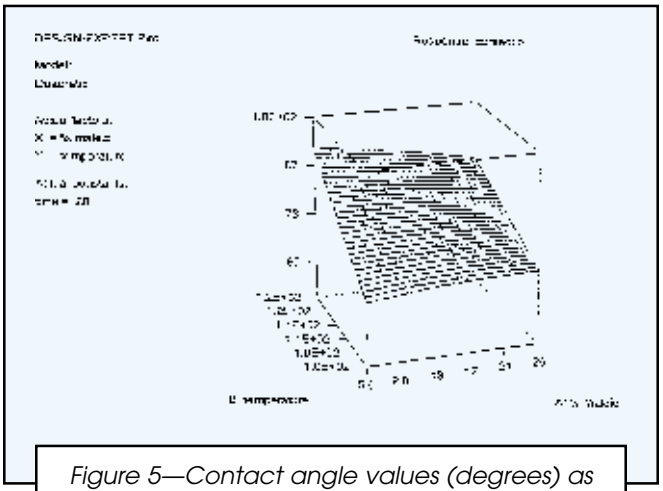

Figure 5—Contact angle values (degrees) as a function of % maleic and bake temperature (°C) at 20 min dry time.

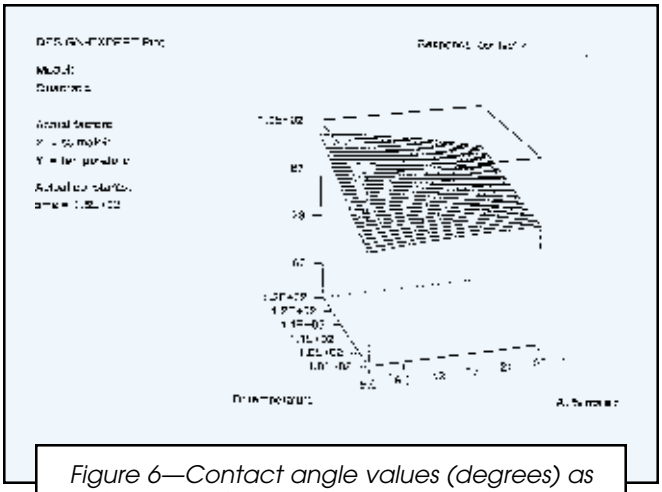

Figure 6—Contact angle values (degrees) as a function of % maleic and bake temperature (°C) at 160 min dry time.

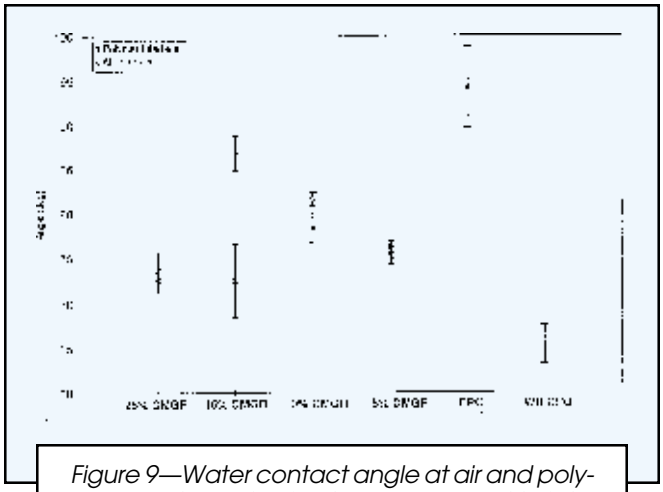

Figure 9—Water contact angle at air and polymer interfaces for CMGR coatings at 80°C for 20 min.

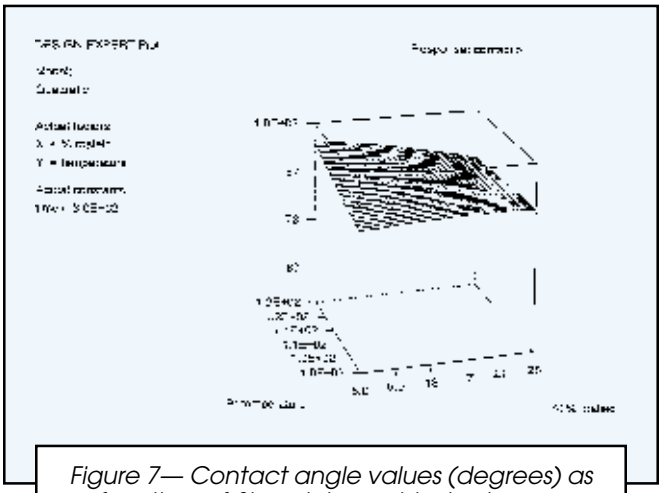

Figure 7— Contact angle values (degrees) as a function of % maleic and bake temperature (°C) at 300 min dry time.

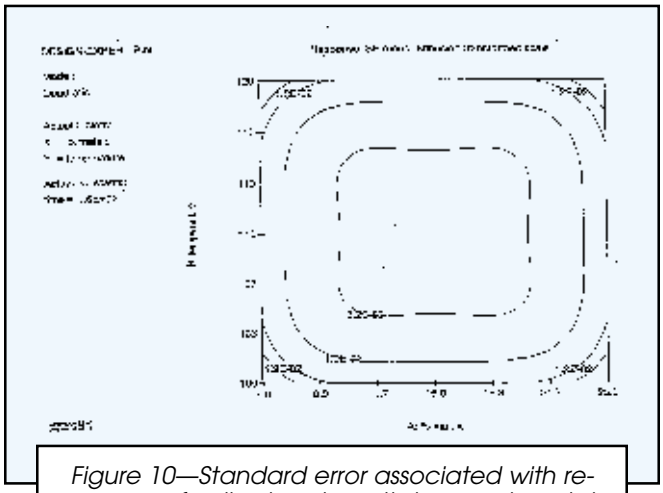

Figure 10—Standard error associated with response of adhesive strength in experimental design.

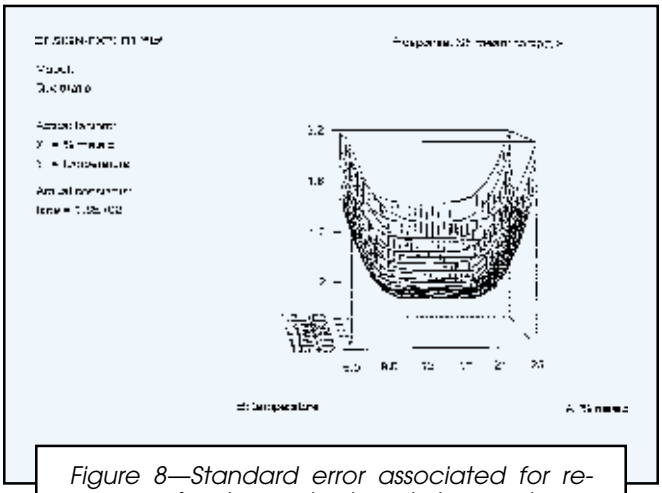

Figure 8—Standard error associated for response of water contact angle in experimental design.

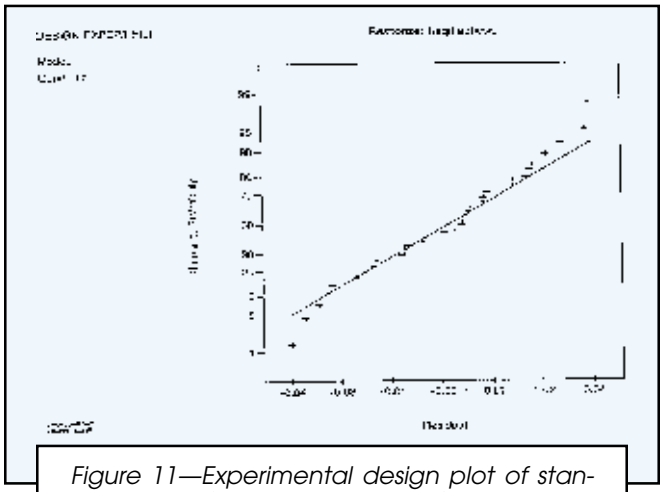

Figure 11—Experimental design plot of standard error of adhesion response (1/square root of adhesion) as a function of % maleic and bake temperature (°C).

Contact Angle and Calculation of the Surface Energy

Contact angle measurements were performed at 20°C. Drops were released from a 26 gauge stainless steel syringe tip with a square end. The precision glass barrel syringes were cleaned in NoChromix® solution and copiously rinsed with distilled water, then rinsed with water distilled from $KMnO_4$. As drops approached surface equilibrium, video frames were recorded and contact angles were digitally measured. The coating-air interface, PP substrate, and the coating-substrate interface after removal from the surface were analyzed. From contact angle values, surface energies were calculated using the Girifalco-Good-Fowkes-Young method shown in equation (3),[2] resident in the FTÅ 200 software.

$$\cos \Theta = \gamma_{sv} - \gamma_{sl}/\gamma \quad (3)$$

RESULTS AND DISCUSSION

CMGR was synthesized at theoretical maleic acid contents of 5, 10, 15, and 25%W/W. The quantity of maleic acid in the polymer was analyzed by FTIR and direct acid-base titration. FTIR absorbance curves as a function of maleic acid content are shown in *Figure* 1. Peak assignments of hydrocarbon C–H (2900 cm^{-1}) and maleic acid show decreasing hydrocarbon and increasing acid group content at higher percent maleinization. In addition, the presence of anhydride functionality was noted for larger percent maleic anhydride by absorbances at 1215 cm^{-1} (C=O), 1778 cm^{-1} (free acid C=O), and 1850 cm^{-1} (O=C–O–C=O).

Titration of acid groups in toluene using standard base in methanol gave the corresponding acid values plotted in *Figure* 2. Correlation of acid value and percent maleinization was observed as 5.5 acid number per theoretical percent maleic anhydride. Reaction efficiency was thus measured at 0.945 equivalents acid per theoretical equivalent maleic acid, or actual slope/theoretical slope. Experimental yields of 100, 88.6, 73.47, and 100% were obtained for theoretical 5, 10, 15, and 25%W/W, respectively. No apparent decrease in reaction efficiency was observed over the range studied.

For an experimental design, the adhesion promoting polymer was formulated into a waterborne coating targeted at 25% VOC, or about 240 g/L (2 lb/gal). Direct aqueous dilution of CMGR solid, either the neutralized salt or the free acid species, was not feasible. However, using a cosolvent to predissolve the neutralized CMGR and subsequent dilution with water permitted formation of a stable aqueous dispersion. THF was an ideal solvent based on moderate volatility, miscibility with water, and excellent CMGR solubility. However, other solvents that were tested as cosolvents failed. For example, DMSO was a good solvent for CMGR at low concentrations (<10%W/W), but lacked the volatility necessary for drying, and at higher CMGR concentrations caused gellation and insolubility. Toluene, a solvent commonly used for CPOs, was a poor solvent for CMGR and further was immiscible with water.

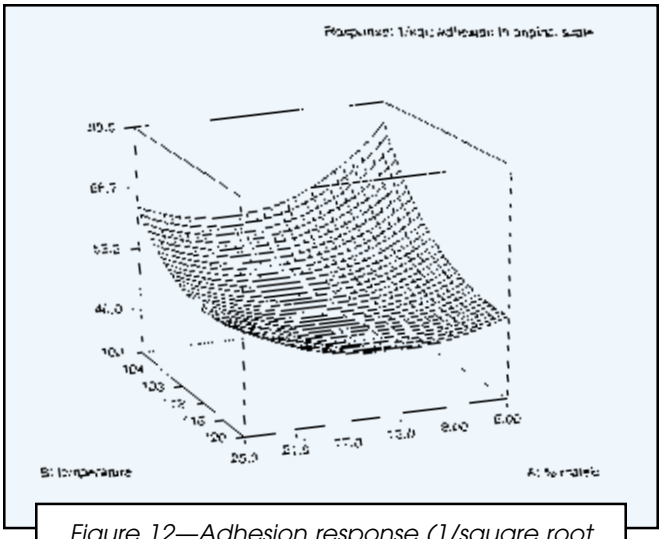

Figure 12—Adhesion response (1/square root of adhesion) as a function of % maleic and bake temperature (°C) at 20 min.

As chlorinated rubbers are hydrophobic, the ability of the coating to remain in aqueous solution is influenced by the percent maleic content. Aqueous dispersions of 5%W/W maleic CMGR were observed to separate after 24 hr. Formulations containing higher maleic anhydride content, showed long-term stability beyond three months with no apparent separation, thus maleic groups were necessary to achieve dispersion stability.

Another concern for coating low energy surfaces was the potential loss of substrate wettability. Poor wetting decreases the substrate area in contact with the coating, reducing adhesion by the ratio of unwetted area to total area[13] and providing loci of adhesion failure cracks. For a coating to wet a surface, the surface tension of the coating must be equal to or less than the substrate surface tension. Water, a high surface tension material and the major coating component, widens the surface energy

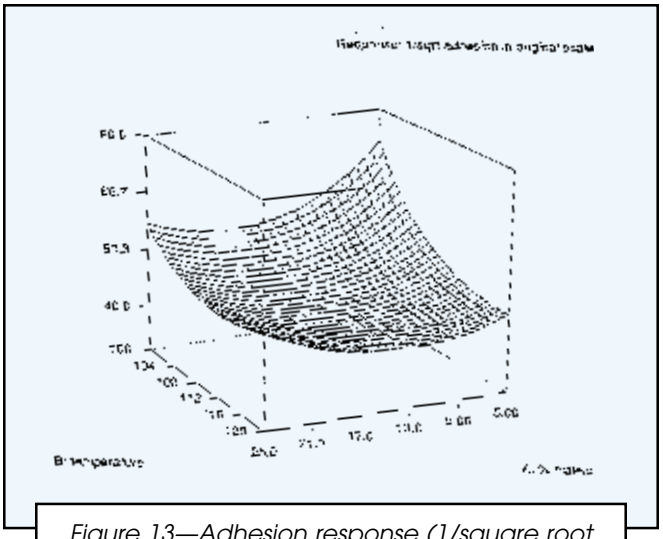

Figure 13—Adhesion response (1/square root of adhesion) as a function of % maleic and bake temperature (°C) at 160 min.

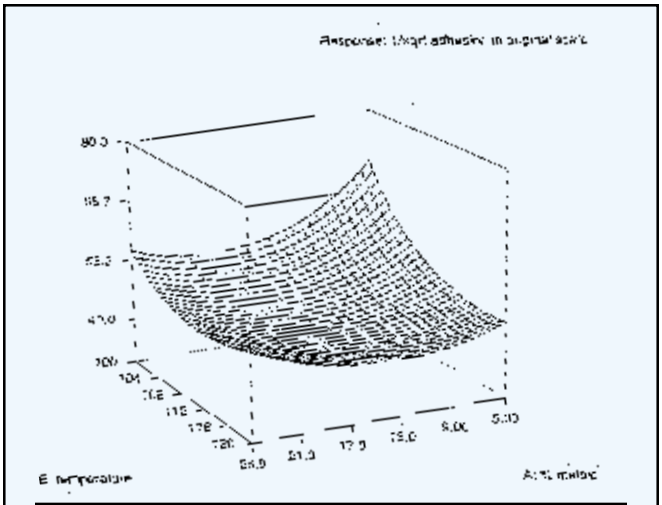

Figure 14—Adhesion response (1/square root of adhesion) as a function of % maleic and bake temperature (°C) at 300 min.

gap between the substrate and coating resulting in poor wetting.

Surfactants form an intimate layer next to a polymeric surface and reduce the energy gap leading to enhanced wetting. Octylphenolethoxylate (CA630) was found to be an adequate surfactant, improving spreading of the film but reducing adhesion. At 0.5% surfactant concentration, the PP surface wettability by the CMGR dispersion increased from approximately 10% surface coverage to complete wetting. The surfactant then migrated to the air interface, thus facilitating waterborne over-coating. Migration of surfactant to the air interface was experimentally verified by ATR FTIR (*Figure* 3), where spectral subtraction of the background absorbance spectrum from each ATR spectrum indicated chlorinated maleinized rubber absorbance in both spectra yet CA630, the added surfactant, only at the air interface (C–O–C, 1100 cm^{-1}).

In the ATR method, light penetration depth into the surface can be calculated using equation (4)[14]:

$$dp = \frac{\lambda_a}{2\pi\sqrt{\cos^2\Theta + \eta_{ab}}} \qquad (4)$$

where depth of penetration (dp) is defined by the wavelength of light (λ_A), the ratio of sample refractive index to that of the crystal (η_{ab}), and the incident angle of the beam as it enters the crystal (Θ). The ATR FTIR spectra of CMGR samples showed absorbances different from CMGR (*Figure* 4) which were attributed to light penetration through the CMGR film and into the substrate surface. The penetration depth using a 45° germanium crystal was 650 nm at maximum penetration (long wavelength) and 100 nm at short wavelength. Although the films were too thin to successfully measure acid group migration at the surface (*Figure* 3), film thickness was shown to be on the order of 100 nm.

Since location/migration of the maleic acid groups could not be distinguished via ATR FTIR, water contact angles were measured. Acid groups increase surface polarity and tension, resulting in a lower contact angle. Thus, components of different surface tensions in coating mixtures orient towards structures that lower systemic free energy.[14]

An experimental design of the variables was made to test the responses of contact angle and adhesion to the change in maleic concentration, drying time, and drying temperature. The response of contact angle was modeled by quadratic interaction terms using no response transformation. The model gave a null probability of 0.5% and a coefficient of variation, equal to root-mean-square error divided by the dependent mean, of less than 5%, indicating a good fit. The model plots obtained for water contact angle at drying times of 20, 160, and 300 min (*Figures* 5-7), respectively, showed contact angle response as a function of all three variables. The response factor equation in coded space was equal to equation (5).

$$\begin{aligned}\text{Contact angle} &= 87.4 \pm 1.2 - (1.4 \pm 0.9)A + (5.8 \pm 0.9)\,B \\ &+ (5.6 \pm 0.9)\,C - (0.7 \pm 1.4)\,A^2 + (0.1 \pm 1.4)\,B^2 \\ &- (3.1 \pm 1.4)\,C^2 - (2.4 \pm 1.1)\,AB - (0.4 \pm 1.1)\,AC \\ &- (4.1 \pm 1.1)\,BC\end{aligned} \qquad (5)$$

where A = %W/W maleic acid, B = dry temperature (°C), and C = dry time (min)

Actual response was equal to equation (6).

$$\begin{aligned}\text{Contact angle} &= -69.2 \pm 2.77A + 1.24B + 0.42C \\ &- 6.7 \times 10^{-3}A^2 + 8.0 \times 10^{-4}B^2 - 1.6 \times 10^{-4}C^2 \\ &- 2.4 \times 10^{-2}AB - 2.7 \times 10^{-4}AC - 3.0 \times 10^{-3}BC\end{aligned} \qquad (6)$$

where A = %W/W maleic acid, B = dry temperature (°C), and C = dry time (min).

In equation (6), factor AC showed no significance within standard error (*Figure* 8) while A showed a small but significant decrease in contact angle. According to the model, the most significant factors to increase contact angle (lower surface tension) were drying temperature and drying time followed by the interaction product of temperature and time (factor BC). Increasing contact angle due to drying time was offset at long times by the negative C^2 term, giving a lower net change due to

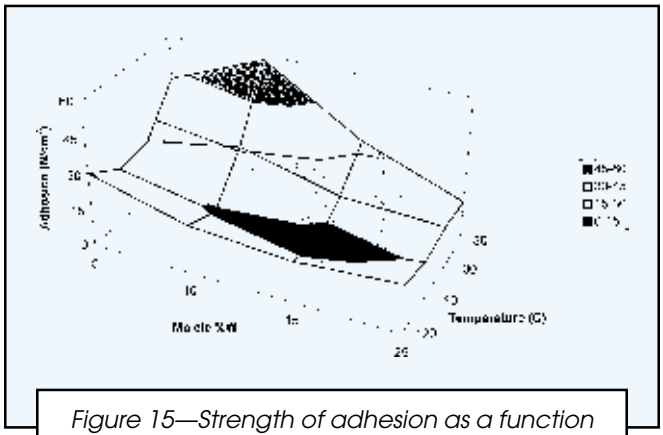

Figure 15—Strength of adhesion as a function of % maleic anhydride and drying temperature with 80°C data.

dry time but leaving a strong temperature and time interaction. Increasing percent maleic acid concentration decreased contact angle slightly, while interaction between maleic acid and temperature decreased contact angle further. Temperature and time effects on contact angle were the result of reduction in water concentration and (unconfirmed) reformation of acid anhydride. The interaction of percent maleic acid and temperature variables indicated a relative change in the mobility of maleic groups within the bulk, and to locate at the surface.

Further proof of the maleic groups' orientation is shown in *Figure* 9. Water contact angle values for air and polymer interfaces as a function of percent maleic concentration increased at the polymer interface with increasing percent maleic acid, though little change occurred at the air interface up to 15%W/W maleic anhydride content. Higher contact angle values indicated hydrophobicity or decreasing presence of maleic groups at the substrate surface. At 25%W/W maleic anhydride content, however, a decreasing contact angle showed a change in maleic orientation where air and PP interfaces possessed polarity.

The effect of maleic orientation on adhesion was then correlated to a change in contact angle, as used earlier in literature.[3] Attempts to model adhesion data without transformation were not useful for generating numerically significant response factors. However, transformation using an inverse square root of response allowed modeling with linear factors to yield one significant factor, drying temperature, within standard error (*Figure* 10). Quadratic model space yielded one additional response factor, percent maleic concentration. The linear model was valid within the null-hypothesis to 57.3% and the coefficient of variance was 17%, while the quadratic model was valid within the null-hypothesis to 18.2% and the coefficient of variance was 18%. Linear coefficients were identical for both models. Large errors for adhesion, from the model as shown in *Figure* 11, were due to range limitations of the load cell used. The response $(\sqrt{\text{adhesion}})^{-1}$ was equal to equation (7):

$$\begin{aligned}(\sqrt{\text{adhesion}})^{-1} &= (0.15 \pm 0.008) + (0.002 \pm 0.006)A \\ &+ (0.009 \pm 0.006)B + (0.002 \pm 0.006)C \\ &- (0.01 \pm 0.009)A^2 - (0.008 + 0.009)B^2 \\ &+ (0.001 \pm 0.009)C^2 - (0.004 + 0.007)AB \\ &+ (0.001 \pm 0.007)AC - (0.001 \pm 0.007)BC\end{aligned} \quad (7)$$

where A = %W/W maleic acid, B = dry temperature (°C), and C = dry time (min)

and the actual response factors were as shown in equation (8):

$$\begin{aligned}(\sqrt{\text{adhesion}})^{-1} &= -1.025 + 7.9 \times 10^{-3}A + 1.92 \times 10^{-2}B \\ &+ 7.64 \times 10^{-5}C - 9.79 \times 10^{-5}A^2 - 7.9 \times 10^{-5}B^2 \\ &+ 3.41 \times 10^{-8}C^2 - 4.43 \times 10^{-5}AB + 4.06 \times \\ &\quad 10^{-7}AC \\ &- 6.91 \times 10^{-7}BC\end{aligned} \quad (8)$$

where A = %W/W maleic acid, B = dry temperature (°C), and C = dry time (min).

Plots of adhesion response over design space are shown in *Figures* 12-14 for drying times of 20, 160, 300 min, respectively. Increasing temperature (B) and the square of percent maleic concentration (A^2) were both observed to decrease adhesion. Higher temperatures possibly degraded the chlorinated compound (~150°C for thermogravimetric onset of CMGR weight loss) causing reduced adhesion. Orientation away from the air surface was supported when water contact angles became constant above 15%W/W maleic anhydride. As has been shown, probing the CMGR to PP interface with water contact angle showed that acid groups began to migrate to the substrate interface at and above 15%W/W maleic anhydride content.

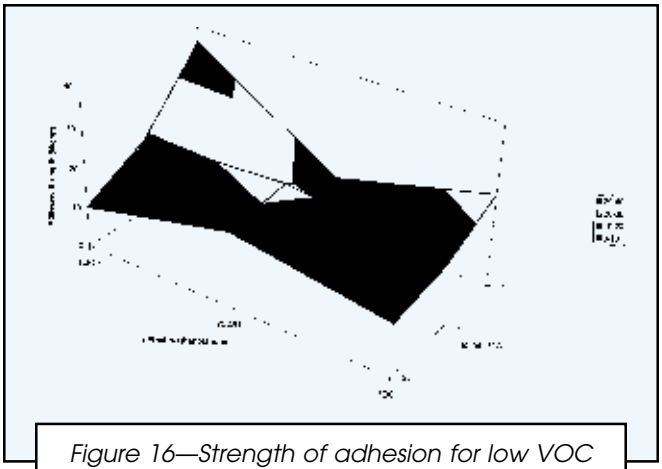

Figure 16—Strength of adhesion for low VOC waterborne CMGR neutralized with ethanolamines.

Since dry time was not significant in either model except through the interaction with temperature, and then the effect was not related to adhesion, a study of even lower dry temperatures was made to further reduce degradation. A composition plot of adhesion as a function of temperature and percent maleic anhydride was obtained (*Figure* 15). Adhesion (57 N/cm^2) was maximized at drying temperatures of 80°C and a CMGR percent maleic anhydride concentration of 10%W/W. A commercial waterborne formulation under identical cure conditions was observed to produce an adhesion of 19 N/cm^2.

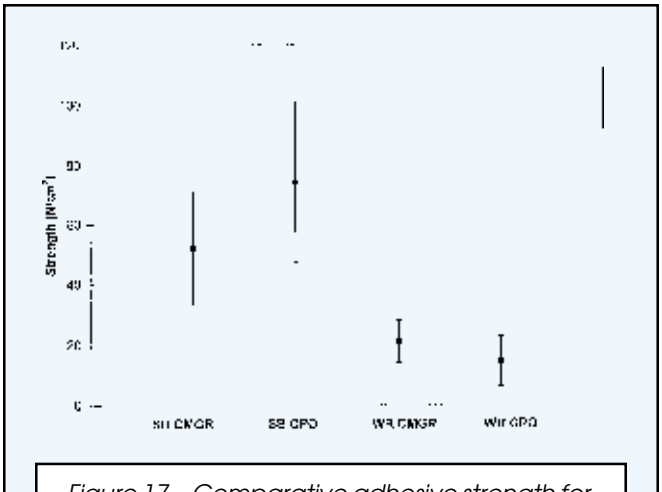

Figure 17—Comparative adhesive strength for SB and WB adhesion promoters.

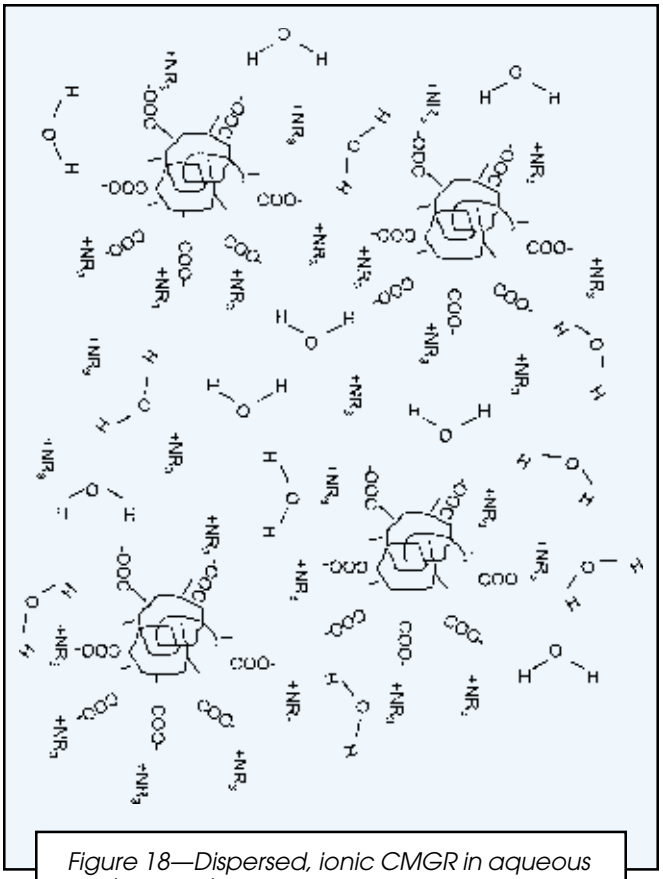

Figure 18—Dispersed, ionic CMGR in aqueous environment.

Though a low VOC (25%) formulation that provided good adhesion (57 N/cm^2) was developed, a still lower VOC formulation was investigated. Although dispersions in lower THF concentration were less stable due to the added hydrophobicity of triethylamine, replacing triethylamine by hydroxyethylamines allowed formation of stable dispersions (*Table* 1). However, adhesion was significantly reduced (*Figure* 16).

Solventborne CMGR formulations were also made (*Table* 1). Adhesion similar to commercial solventborne APs were obtained (~65 N/cm^2). Higher solvent contents thus allowed more efficient orientation of the chlorinated polymer onto the PP substrate, providing better adhesion. An additional benefit apparent from contact angle data was that acidic CMGR provided higher surface tension and improved wettability (*Figure* 17), relative to the solventborne CPO.

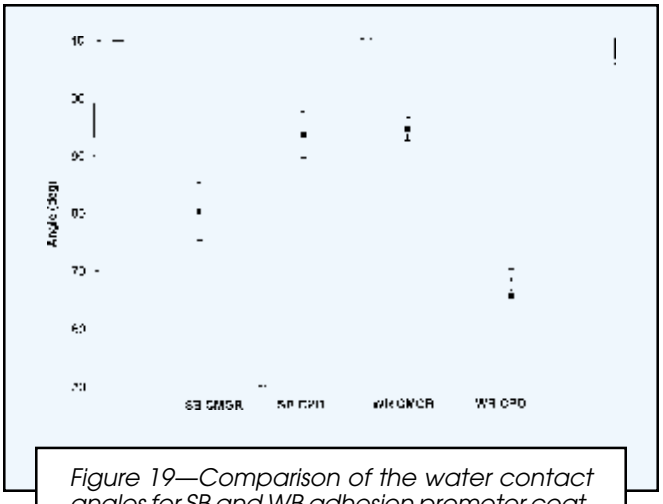

Figure 19—Comparison of the water contact angles for SB and WB adhesion promoter coatings.

Figure 18 shows the adhesion promoter in the water reduced state. However, no adhesion results without the presence of solvent to permit chain adaptation to the nonpolar PP surface. THF allowed uncoiling, better orientation, and adhesion of CMGR to the PP surface in solventborne formulations. The improved ability for orientation is shown in *Figure* 19, where solventborne CMGR of identical maleic content displayed a lower contact angle compared to a waterborne counterpart.

Although solvent swelling plays an important role in adhesion to low energy polymers, this variable was maintained in the waterborne formulations to investigate the effect of the adhesion promoting polymer. When THF concentration was maintained, strength of adhesion varied proving that other influences were affecting adhesion. In *Figure* 15 the THF was incorporated into each of the formulations at 25%W/W yielding variable strengths of adhesion for reasons mentioned previously. If solvent swelling was the only issue to be concerned with, the values for strength of adhesion would have been constant. In waterborne formulations, small quantities of THF enhance adhesion, but not to the same extent as the solventborne counterpart. Finally, no effect in adhesion is expected from the cleaning stage of the PP. The exposure times for the substrate to solvents used to clean them is minimal, 10 to 20 sec. With the high volatile nature of the solvents, the 30 min dry time should be ample for any residual solvent to evaporate.

CONCLUSION

CMGR was formulated into a waterborne coating and proven to work as an adhesion promoter for PP. Contact angle analysis proved to be an effective surface-specific method to qualitatively measure surface migration of components and surface energy. Maximum strength of adhesion was directly related to the amount of solvent, ability of the chlorinated polymer backbone to make intimate contact with the low energy surface, polar content of the polymer (affecting the interfacial surface energies and wettability), and drying temperatures that avoided material degradation of the adhesion promoter. A superior strength of adhesion (57 N/cm^2) for a self-dispersing, water reduced adhesion promoter was obtained at 5-10%W/W maleic anhydride CMGR coating of 240 g/L VOC dried at 80°C, while 10%W/W maleic provided long-term water dispersion stability.

ACKNOWLEDGMENTS

This material was based upon work supported by the Cooperative State Research, Education, and Extension Service, U.S. Department of Agriculture, under Cooperative Agreement No. 93-COOP-1-9530.

Special thanks to Thomas Schuman for assistance with this work and Sharath Mendon for help with the manuscript.

References

(1) (a) Good, R.J., van Oss, C.J., and Chaudhury, M.K., in *Fundamentals of Adhesion*, Lee, L-H. (Ed.), Plenum, New York, 153-179, 1992; (b) van Oss, C.J., Good, R.J., and Chaudhury, M.K., *Langmuir*, 4, 884-891 (1988); (c) van Oss, C.J., Chaudhury, M.K., and Good, R.J., "Monopolar Surfaces," *J. Colloid & Interf. Sci.*, 28, 35-64 (1987).

(2) de Gennes, P.G., "Wetting: Statics and Dynamics," *Rev. Mod. Phys.*, Part 1, 57, 827-863 (1985).

(3) (a) Fowkes, F.M., Riddle, F.L. Jr., Pastore, W.E., and Weber, A.A., *Colloids and Surf.*, 43, 367-378 (1990); (b) Fowkes, F.M., in *Acid-Base Interactions: Relevance to Adhesion Science and Technology*, Mittal, K.L. and Anderson, H.R. Jr., (Eds.), Utrecht, The Netherlands, 47-65, 199, 93-115, 1991; (c) Fowkes, F.M., "Additivity of Intermolecular Forces at Interfaces," *J. Phys. Chem.*, 67, 2538-2541 (1963); (d) Fowkes, F.M., "Attractive Forces at Interfaces," *Ind. Eng. Chem.*, 56, 40 (1964).

(4) Berry, S.R., Rice, S.A., and Ross, J., *Physical Chemistry*, Wiley, New York, 413, 1980.

(5) Alberty, R.A. and Silbey, R., *Physical Chemistry*, First Edition, Wiley-Interscience, New York, 415, 1992.

(6) Sales, A.A., "Dispersion Composition and Method for Making and Using Same," U.S. Patent No. 5 169 888 (1991).

(7) Ainsworth, O.C., "Thermoplastic Elastomers Based upon Chlorosulfonated Polyethylene and a Crystalline Olefin Polymer," U.S. Patent No. 5 387 648 (1993).

(8) Jackson, M.L. et al., "Chlorine-Free, Zero VOC Waterborne Adhesion Promoter for Polyolefinic Substrates," U.S. Patent No. 5 709 946 (1995).

(9) Sharma, M.K., "Waterborne Polyolefin Adhesion Promoter," U.S. Patent No. 5 585 192 (1995).

(10) Toyo Kasei Kogyo, "Modified Polyolefine Resin Coating Compositions," Eur. Patent No. A 080 767 1 (1998).

(11) Ryntz, R.A., "Selection of Weatherable Coatings for Thermoplastic Olefins," JOURNAL OF COATINGS TECHNOLOGY, *63*, No. 799, 63 (1991).

(12) Purvis, W.A. and Thames, S.F., "Chlorinated-Maleinized Guayule Rubber: A Novel Matting Agent for Powder Coatings," JOURNAL OF COATINGS TECHNOLOGY, *68*, No. 857, 67 (1996).

(13) Adamson, A.W. and Gast, A.P., *Physical Chemistry of Surfaces*, Sixth Edition, Wiley-Interscience, New York, 465-470, 1997.

(14) Koenig, J.L., *Spectroscopy of Polymers*, American Chemical Society, Washington, D.C., 47, 1992.

(15) Chattoraj, D.K. and Birdi, K.S., *Adsorption and the Gibbs Surface Excess*, Plenum, New York, 1984.